

**RL-969**

**Acoustic Scattering From Elastic  
Circular Cylinders:  
A Directed Study**

**J. D. Shumpert**

**November 1998**

**RL-969 = RL-969**

# Acoustic Scattering from Elastic Circular Cylinders: A Directed Study

J. D. Shumpert

Radiation Laboratory

Department of Electrical Engineering and Computer Science

The University of Michigan

Ann Arbor, MI 48109-2122

## Abstract

A method for determining the acoustic scattering from elastic circular cylinders is outlined and its salient features discussed. In particular, we are concerned with determining the scattered pressure waves from an infinite solid elastic cylinder immersed in a non-viscous fluid media illuminated by an incident plane wave. The cylinder and surrounding fluid media are described by their acoustic characteristic impedance analogous to the index of refraction from optics or the wave impedance from electromagnetic wave theory. Inside the cylinder, two types of elastic waves are propagated, longitudinal bulk waves traveling in one direction and transverse shear waves traveling at a lower speed and in a different direction.

In order to determine the scattered pressure wave, three boundary conditions must be satisfied, namely, that (i.) the pressure in the fluid must be equal to the normal component of stress in the solid at the surface, (ii.) the normal component of displacement of the fluid must be equal to the normal component of displacement of the solid at the surface, and (iii.) the tangential components of shearing stress must vanish at the surface of the solid. The surface of the cylinder is then simulated using an impedance boundary condition (IBC). First order and second order approximations to the IBC are derived to compare the solution for the scattering from the cylinder obtained using these approximations with the exact solution obtained by matching the boundary conditions exactly at the surface.

The author gratefully acknowledges the support of this research by the National Science Foundation through its Graduate Fellowship Program.

## CONTENTS

I	Introduction	3
II	Biological Media	4
III	Transverse (Shear) Wave Formation	5
IV	Impedance Boundary Conditions	6
V	Accuracy	11
VI	Conclusions	14
A	Appendix – FORTRAN codes	15

## I. INTRODUCTION

One of the fascinating canonical problems that researchers have been interested in for many years is that of computing the acoustic reflection from solid elastic cylinders and spheres immersed in non-viscous fluids. In the straight-forward solution of this problem, one simply treats the body as a scatterer and determines the total field as the sum of the incident field and the scattered field contributed by the body.

The classical problem of determining the acoustic scattering from solid, elastic bodies has been investigated by many researchers using a variety of techniques (the reader is referred to [1] for a comprehensive bibliography of early scattering solution methods). Early research on acoustic scattering from rigid, immovable circular cylinders was carried out by Lord Rayleigh [2]. A more complete solution for rigid cylinders was carried out by Morse and Feshbach [3] in their classic text. Faran [4] solved for the scattered acoustic field from a solid elastic cylinder by matching boundary conditions at the surface and included both longitudinal and shear wave formation. Doolittle and Überall [5] carried the problem further by solving the problem of the scattering from an infinite elastic circular-cylindrical concentric shell, embedded in a fluid and enclosing another fluid. However, each of the above failed to account for losses in the cylinder. Flax and Neubauer [6] derived the theoretical solution for a layered cylindrical shell with absorption. Our solution is exact for elastic cylinders and includes both types of elastic waves and the effect of absorptive processes.

In Section II, parameters such as density and characteristic impedance are defined for specific types of tissue. The formation of the two types of elastic waves propagated inside an elastic body, longitudinal<sup>1</sup> bulk waves traveling at one velocity and transverse<sup>2</sup> shear waves traveling at another velocity, is developed in Section III. Impedance boundary

<sup>1</sup>Throughout this report, various terms are used to represent the two distinct wave propagations in fluids and solids. In the literature the terms *longitudinal* and *compressional* are used interchangeably when describing longitudinal sound waves in a fluid or solid.

<sup>2</sup>The terms *transverse*, *shear*, *distortional*, *equivoluminal*, and *irrotational* are used interchangeably to describe transverse sound waves in a solid.

conditions are derived to simulate the body surface in Section IV. Various approximations to the exact solution are derived and their relative accuracies are shown in Section V. In Section VI applications for these approximate boundary conditions are outlined.

## II. BIOLOGICAL MEDIA

In any material, it is necessary to define parameters that define certain physical properties of that medium. In elastic media, these parameters include the Lamé constants,  $\lambda$  and  $\mu$ , and the density  $\rho$ . Alternatively the media can be described using Poisson's ratio  $\sigma$  and Young's Modulus  $E$  along with the density. The Lamé constants are easily obtained from the longitudinal and shear wave velocities,  $c_1$  and  $c_2$ , as  $\lambda = \rho(c_1^2 - 2c_2^2)$  and  $\mu = \rho c_2^2$ . One of the most important parameters that is used to define biological media is the characteristic impedance  $z$  of a region of an acoustic body which is found by simply multiplying the speed of sound  $c$  in that region with the density of the region

$$z = \rho c = r + jx \quad (1)$$

where  $r$  is the specific acoustic resistance and  $x$  is the specific acoustic reactance. This characteristic impedance is analogous to the index of refraction  $n$  from optics, the wave impedance  $\sqrt{\mu/\epsilon}$  from electromagnetic wave theory, and the characteristic impedance  $Z_o$  from transmission line theory. In Table I is seen various estimates for the speed of sound, density, characteristic impedance, and absorption for various biological material at 1 MHz [7], [8], [9], [10]. HST in Table I refers to Human Soft Tissue, an ensemble parameter average of the different soft tissues for the body. For most soft tissue, the HST value is an acceptable approximation.

Biological media are inherently non-linear and inhomogeneous. This complex media can be simplified by making appropriate assumptions about the media. These simplifications require

1. density fluctuations in the media are small (small condensation)

TABLE I  
VARIOUS BIOLOGICAL PARAMETERS

Tissue	Speed( $c$ ) [m s <sup>-1</sup> ]	Density( $\rho$ ) [g cm <sup>-3</sup> ]	Impedance ( $Z$ ) [10 <sup>6</sup> kg m <sup>-3</sup> s <sup>-1</sup> ]	Absorption( $\alpha$ ) [dB cm <sup>-1</sup> MHz <sup>-1</sup> ]
Blood	1570	1.06	1.61–1.62	0.18
Bone	3360–4080	1.38–1.81	3.75–7.80	13
Brain	1541	1.03	1.55–1.66	0.85
Fat	1450–1476	0.92	1.35–1.38	0.63
Kidney	–	1.04	1.62	–
Liver	1570–1585	1.06	1.64–1.68	–
Lung	650	0.40	0.26	41
Muscle	1568–1585	1.07	1.64–1.74	1.3–3.3
Spleen	–	1.06	1.65–1.67	–
Water	1480	1.00	1.48–1.52	0.0022
Air	343	–	0.000415	12
HST	1540	–	1.63	0.81

2. fluid is homogeneous and isotropic
3. thermal conductivity is very small
4. signal amplitude is small

We also recognize that in any real system, losses must be accounted for. Absorption can be caused by any or all of the following:

1. viscosity of liquid (frictional losses)
2. heat conduction
3. molecular exchanges

### III. TRANSVERSE (SHEAR) WAVE FORMATION

As with any wave theory it is imperative that one characterize the reflection and transmission of the waves at an interface between two different media. In biological acoustics we are concerned with the effect of pressure waves propagating from one fluid to another and the effect of wave reflections from and transmissions through solid interfaces. The reflection and transmission of acoustic waves at a fluid-fluid interface is analogous to that of EM waves interacting at a dielectric interface. One can easily compute the reflection

and transmission coefficients for such an interaction. However, if we now concern ourselves with the reflection and transmission of pressure waves from a elastic solid whose transverse dimension much larger than the wavelength of the acoustic wave, two types of elastic waves are propagated, longitudinal bulk waves traveling in one direction and transverse shear waves traveling at a lower speed and in a different direction.

#### IV. IMPEDANCE BOUNDARY CONDITIONS

The equation of motion of a solid elastic medium is

$$(\lambda + 2\mu)\nabla(\nabla \cdot \mathbf{u}) - \mu\nabla \times (\nabla \times \mathbf{u}) = \rho \frac{\partial^2 \mathbf{u}}{\partial t^2} \quad (2)$$

where  $\mathbf{u}$  is the displacement of the medium. Taking the divergence of both sides of (2) yields the differential equation that the compressional waves satisfy

$$\nabla^2(\nabla \cdot \mathbf{u}) = \frac{\rho}{\lambda + 2\mu} \frac{\partial^2}{\partial t^2} \nabla \cdot \mathbf{u}. \quad (3)$$

Taking the curl of both sides of (2) yields the differential equation that the shear waves satisfy

$$\nabla^2(\nabla \times \mathbf{u}) = \frac{\rho}{\mu} \frac{\partial^2}{\partial t^2} \nabla \times \mathbf{u}. \quad (4)$$

It is convenient to express the displacement  $\mathbf{u}$  as the sum of the gradient of a scalar potential function  $U$  and the curl of a vector function  $\mathbf{A}$

$$\mathbf{u} = -\nabla U + \nabla \times \mathbf{A} \quad (5)$$

where  $U$  represents the compression wave solution and  $\mathbf{A}$  represents the shear wave solution. By introducing potentials  $U$  and  $\mathbf{A}$  we have reduced the problem to that of solving wave equations. In a fluid, we obtain one single wave equation representing a compressional

disturbance. In a solid, we have two waves representing the propagation of a compressional wave at one velocity and a distortional wave at another velocity. If we now define the longitudinal and transverse wave velocities in the elastic body as  $c_1 = \sqrt{(\lambda + 2\mu)/\rho}$  and  $c_2 = \sqrt{\mu/\rho}$ , respectively, then (3) and (4) can be written in a more intuitive form

$$\left(\nabla^2 - \frac{1}{c_1^2} \frac{\partial^2}{\partial t^2}\right) U = 0 \quad (6)$$

$$\left(\nabla^2 - \frac{1}{c_2^2} \frac{\partial^2}{\partial t^2}\right) A_z = 0. \quad (7)$$

For time-harmonic fields ( $e^{j\omega t}$ ), a solution in cylindrical coordinates ( $r, \phi, z$ ) for  $U$  and  $A_z$  can be found from

$$U = \sum_{n=0}^{\infty} \varepsilon_n (-j)^n a_n J_n(k_1 r) \cos n\phi \quad (8)$$

$$A_z = \sum_{n=0}^{\infty} \varepsilon_n (-j)^n b_n J_n(k_2 r) \sin n\phi. \quad (9)$$

where  $k_p = \omega/c_p$  for  $p = 1, 2$ , or  $3$ ,  $\varepsilon_n$  is the Neumann factor, and  $a_n$  and  $b_n$  are unknown coefficients to be determined. The radial and angular components of displacement inside the cylinder can be found from

$$u_r = -\frac{\partial U}{\partial r} + \frac{1}{r} \frac{\partial A_z}{\partial \phi} = \sum_{n=0}^{\infty} \varepsilon_n (-j)^n \left[ \frac{nb_n}{r} J_n(k_2 r) - a_n \frac{d}{dr} J_n(k_1 r) \right] \cos n\phi \quad (10)$$

$$u_\phi = -\frac{1}{r} \frac{\partial U}{\partial \phi} - \frac{\partial A_z}{\partial r} = \sum_{n=0}^{\infty} \varepsilon_n (-j)^n \left[ \frac{na_n}{r} J_n(k_1 r) - b_n \frac{d}{dr} J_n(k_2 r) \right] \sin n\phi. \quad (11)$$



Consider an elastic circular cylinder of radius  $a$  with Lamé constants,  $\lambda$  and  $\mu$ , and density  $\rho$  immersed in a non-viscous fluid media with density  $\rho_3$ . The cylinder is excited by a time-harmonic ( $e^{j\omega t}$ ) incident plane wave

$$p^i = e^{-jk_3x} = e^{-jk_3r \cos \phi} = \sum_{n=0}^{\infty} \varepsilon_n (-j)^n J_n(k_3r) \cos n\phi \quad (12)$$

producing an outward going scattered wave

$$p^s = \sum_{n=0}^{\infty} \varepsilon_n (-j)^n c_n H_n^{(2)}(k_3r) \cos n\phi \quad (13)$$

where  $c_n$  is an unknown coefficient to be determined. If we now define the scattered pressure,  $p$ , in terms of the exterior scalar potential as  $p = -\rho_3\omega^2 U$ , then the radial component of displacement of the incident field is

$$u_r^i = \frac{1}{\rho_3\omega^2} \frac{\partial p_i}{\partial r} = \frac{1}{\rho_3\omega^2} \sum_{n=0}^{\infty} \varepsilon_n (-j)^n \frac{d}{dr} J_n(k_3r) \cos n\phi. \quad (14)$$

The resulting radial component of displacement of the scattered field is

$$u_r^s = \frac{1}{\rho_3\omega^2} \sum_{n=0}^{\infty} \varepsilon_n (-j)^n c_n \frac{d}{dr} H_n^{(2)}(k_3r) \cos n\phi. \quad (15)$$

Note that

$$\nabla \cdot \mathbf{u} = k_1^2 \sum_{n=0}^{\infty} \varepsilon_n (-j)^n a_n J_n(k_1r) \cos n\phi. \quad (16)$$

We can solve for the three unknown coefficients by satisfying three boundary conditions at surface of the solid cylinder. These include

- the pressure in fluid must be equal to the normal component of stress in the solid at the surface  $r = a$

$$p^i + p^s = -[rr] \quad (17)$$

where

$$[rr] = \lambda \nabla \cdot \mathbf{u} + 2\mu \frac{\partial u_r}{\partial r} \quad (18)$$

- the normal component of displacement of the fluid must be equal to the normal component of displacement of the solid at the surface  $r = a$

$$u_r^i + u_r^s = u_r \quad (19)$$

- the tangential components of shearing stress must vanish at the surface  $r = a$

$$[r\phi] = [rz] = 0 \quad (20)$$

where

$$[r\phi] = \mu \left[ \frac{1}{r} \frac{\partial u_r}{\partial \phi} + r \frac{\partial}{\partial r} \left( \frac{u_\phi}{r} \right) \right]$$

$$[rz] = \mu \left[ \frac{\partial u_r}{\partial z} + \frac{\partial u_z}{\partial r} \right]$$

By symmetry,  $[rz] = 0$  everywhere since we have no  $z$  variation and since the exterior fluid supports no shear waves ( $\mu_{\text{fluid}} = 0$ ). Using (20) and substituting (10) and (11) we obtain one equation in  $a_n$  and  $b_n$ . Consequently, we find

$$a_n = \Gamma b_n \quad (21)$$

where

$$\Gamma = \frac{k_2 x_2 J_n''(x_2) - \frac{1}{x_2} J_n'(x_2) + \frac{n^2}{x_2^2} J_n(x_2)}{2nk_1 J_n'(x_1) - \frac{1}{x_1} J_n(x_1)}$$

$$= -\frac{k_2 J'_n(x_2) + \left(\frac{x_2}{2} - \frac{n^2}{x_2}\right) J_n(x_2)}{nk_1 J'_n(x_1) - \frac{1}{x_1} J_n(x_1)} \quad (22)$$

where  $x_p = k_p a$  for  $p = 1, 2$ , or  $3$ . Using (14)–(19), one can solve for  $c_n$  to obtain

$$c_n = -\frac{J_n(x_3) - \eta J'_n(x_3)}{H_n^{(2)}(x_3) - \eta H_n^{\prime(2)}(x_3)} \quad (23)$$

where

$$\eta = \frac{k_3}{\rho_3 \omega^2 a^2} \frac{2\mu n (J_n(x_2) - x_2 J'_n(x_2)) - x_1^2 \Gamma (\lambda J_n(x_1) - 2\mu J''_n(x_1))}{n \frac{k_2}{x_2} J_n(x_2) - k_1 \Gamma J'_n(x_1)} \quad (24)$$

Inserting the expression for  $\Gamma$ , we find

$$\eta = -\frac{k_3 k_1 N}{\rho_3 \omega^2 D} \quad (25)$$

where

$$\begin{aligned} N = & \left(1 - \frac{2n^2}{x_2^2}\right) \left(\lambda + 2\mu - \frac{2\mu n^2}{x_1^2}\right) - \frac{4\mu n^2 k_1}{k_2 x_1^3 x_2} \\ & + \frac{2\mu}{x_1} \left(1 - \frac{2n^2}{x_2^2} + \frac{2n^2 k_1}{k_2 x_1 x_2}\right) \frac{J'_n(x_1)}{J_n(x_1)} \\ & + \frac{2}{x_2} \left(\lambda + 2\mu - \frac{2\mu n^2}{x_1^2} \left(1 - \frac{k_1 x_2}{k_2 x_1}\right)\right) \frac{J'_n(x_2)}{J_n(x_2)} \\ & - 4\mu \frac{k_1}{x_1^2 k_2} \left(n^2 - \frac{k_2 x_1}{k_1 x_1}\right) \frac{J'_n(x_1) J'_n(x_2)}{J_n(x_1) J_n(x_2)} \end{aligned} \quad (26)$$

and

$$D = \left(1 + \frac{2}{x_2} \frac{J'_n(x_2)}{J_n(x_2)}\right) \frac{J'_n(x_1)}{J_n(x_1)} - \frac{2n^2}{x_1 x_2^2} \quad (27)$$

## V. ACCURACY

If  $|x_1|, |x_2|$  are so large that terms  $\mathcal{O}(|x|^{-2})$  can be neglected, then  $J'_n(x) \sim jJ_n(x)$  and

$$N \simeq (\lambda + 2\mu) \left( 1 + \frac{2j}{x_2} + \frac{\mu}{\lambda + 2\mu} \frac{2j}{x_1} \right) \quad (28)$$

$$D \simeq j \left( 1 + \frac{2j}{x_2} \right). \quad (29)$$

If terms  $\mathcal{O}(|x|^{-2})$  are included, but terms  $\mathcal{O}(|x|^{-3})$  are neglected, then

$$J'_n(x) \sim j \left( 1 - \frac{1}{2jx} \right) J_n(x)$$

and

$$N \simeq (\lambda + 2\mu) \left( 1 + \frac{2j}{x_2} \left( 1 - \frac{1}{2jx_2} \right) + \frac{2j}{x_1} \frac{\mu}{\lambda + 2\mu} \left( 1 - \frac{1}{2jx_1} \right) - \frac{2n^2}{x_2^2} - \frac{2n^2}{x_1^2} \frac{\mu}{\lambda + 2\mu} \left( 1 - 2\frac{k_1}{k_2} \right) \right) \quad (30)$$

$$D \simeq j \left( 1 + \frac{2j}{x_2} \left( 1 + \frac{x_2}{4x_1} \right) - \frac{1}{x_2^2} \right). \quad (31)$$

The fact that  $N$  contains terms proportional to  $n^2$  shows that a second order IBC is required.

To illustrate the methods of this directed study and the relative accuracies of the first and second order approximations, we select as a sample structure an infinite elastic cylinder embedded in a “soft” media excited by an incident plane wave. In Figures 1–2 are shown the backscattered far field amplitude for a absorptive cylinder ( $c_1 = 4000$  m/s,  $c_2 = 2500$  m/s,  $\rho = 1.81$  g/cm<sup>3</sup>,  $\alpha_1 = 1 - 4j$ , and  $\alpha_2 = 1 - 4j$ ) immersed in HST<sup>3</sup> ( $c_3 = 1540$  m/s

<sup>3</sup>The HST approximation is selected for the exterior medium and, although not a fluid in the conventional sense, the soft tissue of the body does not permit a shear wave to develop and can therefore be considered a fluid to simplify the numerical computation.

and  $\rho_3 = 1.06 \text{ g/cm}^3$ ). These values correspond to a typical bone segment embedded in soft tissue.

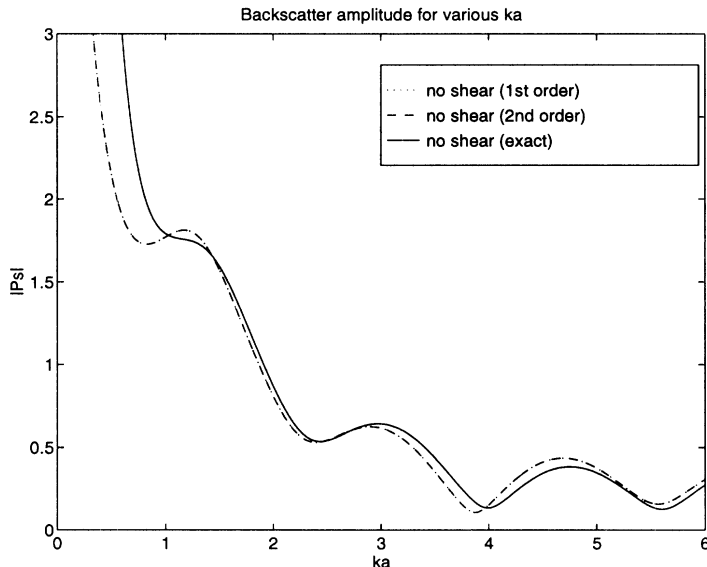


Fig. 1. Backscatter amplitude for various  $ka$  (no shear wave formation)

In Figure 1 is seen the backscattered far field amplitude (with shear wave formation neglected) plotted against  $k_3a$  for the first order approximation ( $\cdots$ ), the second order approximation ( $---$ ), and the exact solution ( $---$ ). Note that the first and second order approximations produce the same backscattered field. This can be explained by simply letting the shear wavelength approach infinity ( $x_2 \rightarrow \infty$ ), or equivalently, letting the shear wave velocity go to zero ( $c_2 \rightarrow 0$ ) and setting  $\mu = 0$  in (26). All of the terms that contain shear information, i.e.  $n^2$  or  $\mu$ , do not contribute to the sum.

If shear waves are then included as seen in Figure 2, the different approximations yield different results. The second order approximation provides an accuracy of 5% if  $k_3a > 0.83$  whereas the first order approximation does not achieve this accuracy until  $k_3a > 2.02$ . As expected, when  $k_3a$  increases, the accuracy of the approximations increase accordingly.

Shear wave formation can have a significant effect on the scattering from small absorptive cylinders. In Figure 3 the exact backscattered far field amplitude is plotted for various  $k_3a$ . As  $k_3a$  increases beyond 25, the effect of the shear waves is reduced significantly.

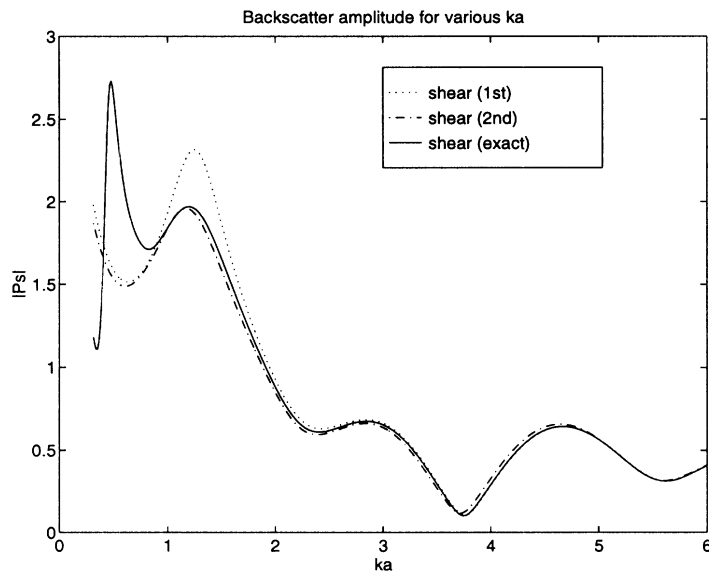


Fig. 2. Backscatter amplitude for various  $ka$  (shear wave formation)

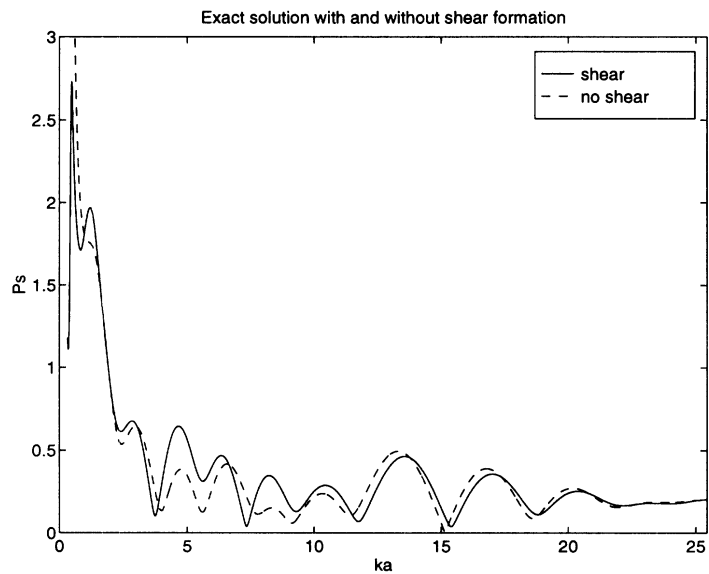


Fig. 3. Backscatter amplitude with and without shear wave formation

Shear wave formation in bone changes the scattering characteristics of ribs or other calcified material. Consequently, the scattering from the ribs during ultrasonic imaging can vary a large amount depending on the frequency used and the placement of the transducers. Since shear wave formation can effect the scattering pattern of the transducer array, it is important to understand and define this transfer of acoustic energy from longitudinal bulk energy to transverse shear energy.

## VI. CONCLUSIONS

In previous work [11], hyperthermia treatment of liver tumors is carried out using a high-intensity optimized ultrasonic synthesized beam. The transducer array is optimized to produce a specific heating pattern at certain points in the body and a minimum at other critical points. A hybrid Ray-Physical Optics (R-PO) technique is employed for the array design. The ribs are considered acoustically “hard” and a reflection coefficient of unity is assigned to each. The certain effect that shear wave formation has on the scattering of the signal through the rib cage is unaccounted for. Future work on this project should include the possible excitation of shear waves and how this can be used to more effectively focus the acoustic energy.

Shear wave formation is a tedious and complicated process to model in complex systems. Simple but effective approximations for the scattering from bodies with different characteristic impedances would aid in producing specific patterns of heating. Impedance boundary conditions are one approximation that can be used to simulate the surface of the rib. For complex systems or bodies these IBCs would provide simple and accurate solutions to the problem of including these shear waves.

## APPENDIX

### I. APPENDIX – FORTRAN CODES

FORTRAN code `acoustic.f`.

```
PROGRAM Acoustic
*
DOUBLE COMPLEX j,k(3),x(3)
DOUBLE COMPLEX Jn1(21),Jn2(21),Jn3(21)
DOUBLE COMPLEX Jn1p(21),Jn2p(21),Jn3p(21)
DOUBLE COMPLEX Yn1(21),Yn2(21),Yn3(21)
DOUBLE COMPLEX Yn1p(21),Yn2p(21),Yn3p(21)
DOUBLE COMPLEX Hn3(21),Hn3p(21)
DOUBLE PRECISION c(3),p(3),lame(2),w,alpha(3),lambda(3)
DOUBLE PRECISION a,pi,neumann(21),K1,K2,f
DOUBLE COMPLEX Gamma,num,den,eta,sum,c_n
DOUBLE COMPLEX p_s(4,300)
INTEGER i,m,iter,N
COMMON /Arg/ x
DATA f /1.d6/

* Calculate the needed constants for the cylinder and fluid

WRITE (*,*) 'Lucite (1) or Bone (2)'
READ (*,*) idno1
IF (idno1.eq.1) THEN
    c(1)=2680.d0
    c(2)=1380.d0
    c(3)=482.d0
    p(1)=1.18d3
    p(2)=1.18d3
```



```

p(3)=0.998d3
WRITE (*,*) 'Attenuation (1) or No attenuation (2)'
READ (*,*) idno2
IF (idno2.eq.1) THEN
    alpha(1)=1.0068d1
    alpha(2)=1.0102d1
    alpha(3)=0.0d0
ELSE
    alpha(1)=0.0d0
    alpha(2)=0.0d0
    alpha(3)=0.0d0
ENDIF
ELSE
c(1)=4000.d0
c(2)=2000.d0
c(3)=1540.d0
p(1)=1.81d3
p(2)=1.81d3
p(3)=1.07d3
WRITE (*,*) 'Attenuation (1) or No attenuation (2)'
READ (*,*) idno2
IF (idno2.eq.1) THEN
    alpha(1)=2.0d0
    alpha(2)=2.0d0
    alpha(3)=0.0d0
ELSE
    alpha(1)=0.0d0
    alpha(2)=0.0d0
    alpha(3)=0.0d0

```

```

        ENDIF
ENDIF
DATA pi /3.1415926535897932d0/
*   DATA a /1.54e-3/
DATA j /(0.d0,1.d0)/
OPEN (UNIT=1,FILE='exact.dat')
OPEN (UNIT=2,FILE='first.dat')
OPEN (UNIT=3,FILE='second.dat')
OPEN (UNIT=4,FILE='exact2.dat')
N=21
w=2.d0*pi*f
lame(1)=p(1)*(c(1)**2-2.*c(2)**2)
lame(2)=p(1)*c(2)**2
DO i=1,3
    lambda(i)=c(i)/f
    k(i)=2.d0*pi/lambda(i)*(1.d0-j*alpha(i))
ENDDO
a0=lambda(3)
delta=a0/100.d0
DO iter=1,200
    a=0.05*a0+DFLOAT(iter-1)*delta
    DO i=1,3
        x(i)=k(i)*a
    ENDDO
    neumann(1)=1.d0
    DO m=2,N
        neumann(m)=2.d0
    ENDDO
* Calculate Bessel tables for summation

```

```

CALL Getj(N, Jn1, Jn2, Jn3)
CALL Getjp(N, Jn1p, Jn2p, Jn3p, Jn1, Jn2, Jn3)
CALL Gety(N, Yn1, Yn2, Yn3)
CALL Getyp(N, Yn1p, Yn2p, Yn3p, Yn1, Yn2, Yn3)
CALL Geth(N, Jn3, Yn3, Hn3)
CALL Gethp(N, Hn3p, Hn3)

* Calculate exact solution #1

*      sum=0.
*      DO m=1, N-1
*          Gamma=-k(2)/(DFLOAT(m)*k(1))*(Jn2p(m)+(x(2)/2.d0-
*      +          DFLOAT(m)**2/x(2))*Jn2(m))/
*      +          (Jn1p(m)-Jn1(m)/x(1))
*          num=2.d0*lame(2)*DFLOAT(m)*(Jn2(m)-
*      +          x(2)*Jn2p(m))-x(1)**2*
*      +          Gamma*((lame(1)+2.d0*lame(2)*
*      +          (1.d0-DFLOAT(m)**2/x(1)**2))*
*      +          Jn1(m)+2.d0*lame(2)/x(1)*Jn1p(m))
*          den=DFLOAT(m)*k(2)/x(2)*Jn2(m)-k(1)*Gamma*Jn1p(m)
*          eta=k(3)/(p(3)*w**2*a**2)*num/den
*          c_n=- (Jn3(m)-eta*Jn3p(m))/(Hn3(m)-eta*Hn3p(m))
*          sum=sum+neumann(m)*(-j)**m*c_n
*      ENDDO
*      p_s(3, iter)=sum*DSQRT(2.d0/(pi*x(3)))

```

```

* Calculate exact solution #2

```

```

sum=0.
K1=lame(1)+2.d0*lame(2)
DO m=1, N-1

```

```

Gamma=-k(2)/(DFLOAT(m)*k(1))*(Jn2p(m)+(x(2)/2.d0
+      -DFLOAT(m)**2/x(2))*Jn2(m))/
+      (Jn1p(m)-Jn1(m)/x(1))
num=(1.d0-2.d0*2.d0*DFLOAT(m)**2/x(2)**2)*
+      (K1-2.d0*lame(2)*
+      DFLOAT(m)**2/x(1)**2)-4.d0*lame(2)*
+      DFLOAT(m)**2*k(1)/(k(2)*x(1)**3*x(2))+
+      2.d0*lame(2)/x(1)*(1.d0-2.d0*DFLOAT(m)**2/
+      x(2)**2+2.d0*DFLOAT(m)**2*k(1)/
+      (k(2)*x(1)*x(2)))*Jn1p(m)/Jn1(m)+
+      2.d0/x(2)*(K1-2.d0*lame(2)*
+      DFLOAT(m)**2/x(1)**2*
+      (1.d0-k(1)*x(2)/(k(2)*x(1))))*Jn2p(m)/Jn2(m)-
+      4.d0*lame(2)*k(1)/(x(1)**2*k(2))*
+      (DFLOAT(m)**2-k(2)*x(1)/(k(1)*x(2)))*
+      Jn2p(m)/Jn2(m)*Jn1p(m)/Jn1(m)
den=(1.d0+2.d0/x(2)*Jn2p(m)/Jn2(m))*Jn1p(m)/Jn1(m)-
+      2.d0*DFLOAT(m)**2/(x(1)*x(2)**2)
eta=-k(1)*k(3)/(p(3)*w**2)*num/den
c_n=- (Jn3(m)-eta*Jn3p(m))/(Hn3(m)-eta*Hn3p(m))
sum=sum+neumann(m)*(-j)**m*c_n
ENDDO
p_s(4,iter)=sum*DSQRT(2.d0/(pi*x(3)))

```

\* Calculate 1st order solution

```

sum=0.
DO m=1,N-1
  K1=lame(1)+2.d0*lame(2)
  K2=lame(2)/K1

```

```

num=K1*(1.d0+2.d0*j/x(2)+K2*2.d0*j/x(1))
den=j*(1.d0+2.d0*j/x(2))
eta=-k(3)*k(1)/(p(3)*w**2)*num/den
c_n=-(Jn3(m)-eta*Jn3p(m))/(Hn3(m)-eta*Hn3p(m))
sum=sum+neumann(m)*(-j)**m*c_n
ENDDO
p_s(1,iter)=sum*DSQRT(2.d0/(pi*x(3)))

```

\* Calculate 2nd order solution

```

sum=0.
DO m=1,N-1
  K1=lame(1)+2.d0*lame(2)
  K2=lame(2)/K1
  num=K1*(1.d0+2.d0*j/x(2)*(1.d0-1.d0/(2.d0*j*x(2))))
+   +2.d0*j/x(1)*K2*(1.d0-1.d0/(2.d0*j*x(1)))
+   -2.d0*DFLOAT(m)**2/x(2)**2-2.d0*DFLOAT(m)**2
+   /x(1)**2*K2*(1.d0-2.d0*k(1)/k(2))
  den=j*(1.d0+2.d0*j/x(2)*(1.d0+x(2)/(4.d0*x(1))))
+   -1.d0/x(2)**2)
  eta=-k(3)*k(1)/(p(3)*w**2)*num/den
  c_n=-(Jn3(m)-eta*Jn3p(m))/(Hn3(m)-eta*Hn3p(m))
  sum=sum+neumann(m)*(-j)**m*c_n
ENDDO
p_s(2,iter)=sum*DSQRT(2.d0/(pi*x(3)))
WRITE (1,*) real(k(3)*a),abs(p_s(3,iter))
WRITE (2,*) abs(p_s(1,iter))
WRITE (3,*) abs(p_s(2,iter))
WRITE (4,*) abs(p_s(4,iter))
ENDDO

```

STOP

END

```
*
*
***** Bessel Subroutines *****
*
```

SUBROUTINE Getj(N,Jn1,Jn2,Jn3)

\* Calculate J(X1), J(X2), and J(X3)

DOUBLE COMPLEX x(3),j

DOUBLE COMPLEX Jn1(21),Jn2(21),Jn3(21)

DOUBLE PRECISION Dyr(21),Dyi(21),Zr,Zi

INTEGER i,m

COMMON /Arg/ x

DATA j /(0.d0,1.d0)/

DO i=1,3

    Zr=REAL(x(i))

    Zi=AIMAG(x(i))

    CALL Zbesj(Zr,Zi,0.d0,1,N,Dyr,Dyi,Nz,Ierr)

    IF (Ierr.NE.0) WRITE (\*,\*) Ierr

    IF (i.EQ.1) THEN

        DO m=1,N

            Jn1(m)=Dyr(m)+j\*Dyi(m)

        ENDDO

    ELSEIF (i.EQ.2) THEN

        DO m=1,N

            Jn2(m)=Dyr(m)+j\*Dyi(m)

        ENDDO

    ELSE

        DO m=1,N

```

        Jn3(m)=Dyr(m)+j*Dyi(m)
    ENDDO
ENDIF
ENDDO
RETURN
END

SUBROUTINE Getjp(N, Jn1p, Jn2p, Jn3p, Jn1, Jn2, Jn3)

```

\* Calculate  $J'(X_1)$ ,  $J'(X_2)$ , and  $J'(X_3)$

```

DOUBLE COMPLEX x(3)
DOUBLE COMPLEX Jn1p(21), Jn2p(21), Jn3p(21)
DOUBLE COMPLEX Jn1(21), Jn2(21), Jn3(21)
INTEGER i, m
COMMON /Arg/ x
DO i=1,3
    IF (i.eq.1) THEN
        DO m=1, N-1
            Jn1p(m)=-Jn1(m+1)+DFLOAT(m)/x(1)*Jn1(m)
        ENDDO
    ELSEIF (i.eq.2) THEN
        DO m=1, N-1
            Jn2p(m)=-Jn2(m+1)+DFLOAT(m)/x(2)*Jn2(m)
        ENDDO
    ELSE
        DO m=1, N-1
            Jn3p(m)=-Jn3(m+1)+DFLOAT(m)/x(3)*Jn3(m)
        ENDDO
    ENDIF
ENDDO

```

RETURN

END

SUBROUTINE Gety(N,Yn1,Yn2,Yn3)

\* Calculate Y(X1), Y(X2), and Y(X3)

DOUBLE COMPLEX x(3),j

DOUBLE COMPLEX Yn1(21),Yn2(21),Yn3(21)

DOUBLE PRECISION Dyr(21),Dyi(21),Zr,Zi

DOUBLE PRECISION Dwrkr(21),Dwrki(21)

INTEGER i,m

COMMON /Arg/ x

DATA j /(0.d0,1.d0)/

DO i=1,3

    Zr=REAL(x(i))

    Zi=AIMAG(x(i))

    CALL Zbesy(Zr,Zi,0.d0,1,N,Dyr,Dyi,Nz,dwrkr,dwrki,Ierr)

    IF (Ierr.NE.0) WRITE (\*,\*) Ierr

    IF (i.eq.1) THEN

        DO m=1,N

            Yn1(m)=Dyr(m)+j\*Dyi(m)

        ENDDO

    ELSEIF (i.eq.2) THEN

        DO m=1,N

            Yn2(m)=Dyr(m)+j\*Dyi(m)

        ENDDO

    ELSE

        DO m=1,N

            Yn3(m)=Dyr(m)+j\*Dyi(m)

        ENDDO



```

ENDIF
ENDDO
RETURN
END

```

```

SUBROUTINE Getyp(N,Yn1p,Yn2p,Yn3p,Yn1,Yn2,Yn3)

```

```

* Calculate Y'(X1), Y'(X2), and Y'(X3)

```

```

DOUBLE COMPLEX x(3)
DOUBLE COMPLEX Yn1p(21),Yn2p(21),Yn3p(21)
DOUBLE COMPLEX Yn1(21),Yn2(21),Yn3(21)
INTEGER i,m
COMMON /Arg/ x
DO i=1,3
  IF (i.eq.1) THEN
    DO m=1,N-1
      Yn1p(m)=-Yn1(m+1)+DFLOAT(m)/x(1)*Yn1(m)
    ENDDO
  ELSEIF (i.eq.2) THEN
    DO m=1,N-1
      Yn2p(m)=-Yn2(m+1)+DFLOAT(m)/x(2)*Yn2(m)
    ENDDO
  ELSE
    DO m=1,N-1
      Yn3p(m)=-Yn3(m+1)+DFLOAT(m)/x(3)*Yn3(m)
    ENDDO
  ENDIF
ENDDO
RETURN
END

```

```
SUBROUTINE Geth(N, Jn3, Yn3, Hn3)
```

```
* Calculate Hn_2(X3)
```

```
DOUBLE COMPLEX Jn3(21), Yn3(21), Hn3(21), j
```

```
INTEGER m
```

```
DATA j / (0.d0, 1.d0) /
```

```
DO m=1, N
```

```
    Hn3(m) = Jn3(m) - j * Yn3(m)
```

```
ENDDO
```

```
RETURN
```

```
END
```

```
SUBROUTINE Gethp(N, Hn3p, Hn3)
```

```
* Calculate Hn'_2(X3)
```

```
DOUBLE COMPLEX x(3)
```

```
DOUBLE COMPLEX Hn3p(21), Hn3(21)
```

```
INTEGER i, m
```

```
COMMON /Arg/ x
```

```
DO i=3, 3
```

```
    DO m=1, N-1
```

```
        Hn3p(m) = -Hn3(m+1) + DFLOAT(m) / x(3) * Hn3(m)
```

```
    ENDDO
```

```
ENDDO
```

```
RETURN
```

```
END
```

## REFERENCES

- [1] N. A. Logan, "Survey of some early studies of the scattering of plane waves by a sphere," *Proc. IEEE*, vol. 53, no. 8, pp. 773–785, Aug 1965.
- [2] J. W. Strutt (Lord Rayleigh), *Theory of Sound*, MacMillan, London, 1878.
- [3] P. M. Morse and H. Feshbach, *Methods of Theoretical Physics*, McGraw-Hill, London, 1953.
- [4] J. J. Faran, "Sound scattering by solid cylinders and spheres," *J. Acous. Soc. Amer.*, vol. 23, no. 4, pp. 405–418, July 1951.
- [5] R. D. Doolittle and H. Überall, "Sound scattering by elastic cylindrical shells," *J. Acous. Soc. Amer.*, vol. 39, no. 2, pp. 272–275, 1966.
- [6] L. Flax and W. G. Neubauer, "Acoustic reflection from layered elastic absorptive cylinders," *J. Acous. Soc. Amer.*, vol. 61, no. 2, pp. 307–312, Feb 1977.
- [7] D. E. Goldman and T. F. Heuter, "Tabular data of the velocity of high-frequency sound in mammalian tissue," *J. Acous. Soc. Amer.*, vol. 28, pp. 37–37, 1956.
- [8] P. N. T. Wells, *Biomedical Ultrasonics*, Academic Press, London, 1977.
- [9] R. C. Chivers, "Ultrasonic velocity and attenuation in mammalian tissues," *J. Acous. Soc. Amer.*, vol. 63, pp. 940–953, 1978.
- [10] J. P. Jones, "Quantitative characterization of tissue using ultrasound," *IEEE Trans. Nucl. Sci.*, vol. NS-27, no. 3, Jun 1980.
- [11] Y. Y. Botros, *Optimal phased array pattern synthesis for non-invasive cancer ablation of liver tumors using high intensity focused ultrasound*, Ph.D. thesis, The University of Michigan, 1998.
- [12] L. E. Kinsler, *Fundamentals of Acoustics*, John Wiley & Sons, New York, NY, third edition, 1982.
- [13] T. B. A. Senior and J. L. Volakis, *Approximate Boundary Conditions in Electromagnetics*, IEE Press, London, 1995.
- [14] T. B. A. Senior, "Generalized boundary conditions for scalar fields," *J. Acous. Soc. Amer.*, vol. 97, no. 6, pp. 3473–3477, Jun 1995.

# Impedance Boundary Conditions in Ultrasonics

John D. Shumpert and Thomas B. A. Senior

Radiation Laboratory  
Department of Electrical Engineering and Computer Science  
University of Michigan  
Ann Arbor, Michigan 48109-2122 USA

September 1999

## Abstract

A generalized impedance boundary condition (GIBC) is developed to approximate the scattering of a plane acoustic wave from a bone structure such as a rib. In particular, the rib and surrounding tissue are modeled as a viscoelastic cylinder of infinite length immersed in an infinite, inviscid fluid media. In order to determine the scattered pressure wave, appropriate boundary conditions are imposed on the relevant differential equations at the fluid-solid surface. The exact solution is then used to develop first and second order impedance boundary conditions applicable at the surface of the cylinder. Numerical results demonstrate the improved accuracy of the second order condition.

## 1 INTRODUCTION

A problem of interest in bioengineering is the scattering of acoustic waves from bone structures such as the rib cage. For biomedical applications, a particular concern is the effect of pressure waves propagating from one fluid to another and the effect of shear wave formation in the more solid regions of the body, such as bone. Even though bone and other calcified material are neither solid nor homogeneous, they are capable of supporting both shear and compressional waves. This is in contrast to the background tissue surrounding the rib cage. This tissue is soft and reasonably homogeneous but does not permit a shear wave to develop. From a consideration of the material properties of bone and soft tissue at the frequencies of concern, it is clear that the porous bone structure may be modeled as a viscoelastic medium and the soft tissue as a fluid.

In order to appropriately model the bone and soft tissue structures, various parameter estimates for the speed of sound, material density, characteristic impedance, and absorption, are

listed in Table I [1, 2, 3, 4]. For an operating frequency of 1 MHz, the corresponding acoustic wavelength inside the rib is 4 mm. HST refers to Human Soft Tissue, an ensemble parameter average of the different soft tissues for the body. For most soft tissues, the HST value is an acceptable approximation. As can be seen, acoustic absorption in human tissue occurring through natural viscosity, heat conduction, and/or molecular exchanges can be significant and must be accounted for.

The reflection and transmission of acoustic waves at a fluid-fluid interface is analogous to that of electromagnetic waves interacting at a dielectric interface. It is a straight-forward procedure to compute the reflection and transmission coefficients for a variety of simple shapes [5]. However, if we now concern ourselves with the reflection and transmission of pressure waves from an elastic solid, two types of elastic waves are propagated, longitudinal bulk waves traveling in one direction and transverse shear waves traveling at a lower speed and in a different direction. Elastic media can be described using the Lamé constants,  $\lambda$  and  $\mu$ , and the density  $\rho$ , or alternatively, using Young's Modulus  $E$  and Poisson's ratio  $\sigma$  along with the density. An important parameter that is used in defining acoustic media is the specific acoustic impedance  $Z$ , defined as the ratio of acoustic pressure to the normal particle velocity at the surface. For our purposes, however, it is more convenient to employ the reciprocal of the impedance, *i.e.*, the specific acoustic admittance  $Y$ . For plane acoustic waves, the impedance of the wave can be found from the product of the density  $\rho$  and the wave speed  $c$  in the medium.

One of the first complete treatments of elastic scattering from cylinders and spheres was carried out by Faran [6], but no attention was paid to viscous losses. Vogt *et al.* [7, 8] were one of the first groups to determine the reflection of a plane wave from an absorbing sphere. Flax and Neubauer [9] derived a solution for a layered cylindrical shell with absorption. Many of the early solutions [10] assumed the specific acoustic impedance was constant for all partial-wave modes of the body, equivalent to using a first order (or standard) impedance boundary condition (SIBC). Parametric studies were carried out to determine an appropriate value for this impedance, but as noted by Ayres and Gaunard [11], the assumption of a constant impedance is inadequate. The specific acoustic impedance is frequency dependent and depends not only on the material parameters but is also a function of the partial-wave index  $n$ .

The simplest canonical shape that bears a resemblance to a rib is a circular cylinder, and the problem considered here is the scattering of a plane acoustic wave incident on a homogeneous viscoelastic cylinder of infinite length immersed in an inviscid fluid. The exact solution is obtained in the form of an eigenfunction expansion, and the specific acoustic admittance of each partial mode is determined. The solution is then used to develop first and second order impedance boundary conditions applicable at the surface of the cylinder. It would appear that this is the first time that second order conditions have been considered in the context of viscoelastic media, but in electromagnetics impedance boundary conditions have a rich history. In particular, Wait explored at length the use of SIBCs in propagation and scattering problems (see, for example, [12]). An SIBC is developed in Section 3.1 and a second order generalized impedance boundary condition (GIBC) in Section 3.2, and their accuracy is determined by comparison with the exact solution. Such boundary conditions have the advantage of converting a two media problem into a single medium one, and since an actual rib is not circular in cross section, they may be helpful in the numerical solution for a more realistic geometry.

## 2 FORMULATION OF SOLUTION

In the straight-forward solution of this problem, one treats the body as a scatterer and determines the total field as the sum of the incident field and the scattered field contributed by the body. Following Faran [6], we consider an infinite elastic circular cylinder of radius  $a$ , Young's modulus  $E$ , Poisson's ratio  $\sigma$ , and density  $\rho$  immersed in an inviscid fluid media with density  $\rho_0$ . The cylinder (see Fig. 1) is excited by a time-harmonic ( $e^{j\omega t}$ ) incident acoustic plane wave of the form

$$p^i = P_0 e^{-jk_0 x} = P_0 e^{-jk_0 r \cos \phi} = P_0 \sum_{n=0}^{\infty} \varepsilon_n j^{-n} J_n(k_0 r) \cos n\phi \quad (1)$$

producing an outward going scattered acoustic wave

$$p^s = P_0 \sum_{n=0}^{\infty} \varepsilon_n j^{-n} c_n H_n^{(2)}(k_0 r) \cos n\phi \quad (2)$$

where  $c_n$  is an unknown coefficient to be determined.

The equation of motion of a solid elastic medium is given by Love [13]

$$\frac{E(1-\sigma)}{(1+\sigma)(1-2\sigma)}\nabla(\nabla\cdot\mathbf{u})-\frac{E}{2(1+\sigma)}\nabla\times(\nabla\times\mathbf{u})=\rho\frac{\partial^2\mathbf{u}}{\partial t^2} \quad (3)$$

where (3) has been written in terms of  $E$ , and  $\sigma$ , and the particle displacement  $\mathbf{u}$ . Taking the divergence of both sides of (3) yields the differential equation that the compressional wave solution satisfies; taking the curl of both sides of (3) yields the differential equation that the shear wave solution satisfies. The displacement can be expressed as the sum of the gradient of a scalar potential function  $U$  and the curl of a vector potential function  $\mathbf{A}$  [14]

$$\mathbf{u}=-\nabla U+\nabla\times\mathbf{A} \quad (4)$$

where  $U$  represents the compression wave solution and  $\mathbf{A}$  the shear wave solution. For two-dimensional problems, where  $\mathbf{A}$  has only a  $z$  component, the potentials satisfy the scalar wave equations

$$\left(\nabla^2-\frac{1}{c_1^2}\frac{\partial^2}{\partial t^2}\right)U=0 \quad (5a)$$

$$\left(\nabla^2-\frac{1}{c_2^2}\frac{\partial^2}{\partial t^2}\right)A_z=0 \quad (5b)$$

where the longitudinal and transverse wave velocities in the elastic body are expressed, respectively, as

$$c_1=\sqrt{\frac{E(1-\sigma)}{\rho(1+\sigma)(1-2\sigma)}}=\sqrt{\frac{\lambda+2\mu}{\rho}}$$

$$c_2=\sqrt{\frac{E}{2\rho(1+\sigma)}}=\sqrt{\frac{\mu}{\rho}}.$$

Solutions in cylindrical coordinates  $(r, \phi, z)$  for  $U$  and  $A_z$  are

$$U=P_0\sum_{n=0}^{\infty}\varepsilon_n j^{-n}a_n J_n(k_1 r)\cos n\phi \quad (6a)$$

$$A_z=P_0\sum_{n=0}^{\infty}\varepsilon_n j^{-n}b_n J_n(k_2 r)\sin n\phi. \quad (6b)$$

where  $k_p = \omega/c_p$  for  $p = 0, 1$ , or  $2$ ,  $\varepsilon_n$  is the Neumann factor, and  $a_n$  and  $b_n$  are unknown coefficients to be determined. Throughout this work, the subscript 0 refers to the external fluid,

and subscripts 1 and 2 to the longitudinal and transverse components of the viscoelastic medium, respectively.

## 2.1 Elastic Media

Three boundary conditions must be satisfied at the surface of the cylinder:

- the pressure in the fluid must be equal to the normal component of stress  $e_{rr}$  on the solid at the surface  $r = a$

$$p^i + p^s = -e_{rr} \quad (7a)$$

where

$$e_{rr} = \frac{E\sigma}{(1+\sigma)(1-2\sigma)} \nabla \cdot \mathbf{u} + \frac{E}{1+\sigma} \frac{\partial u_r}{\partial r} \quad (7b)$$

with

$$\nabla \cdot \mathbf{u} = P_0 k_1^2 \sum_{n=0}^{\infty} \varepsilon_n j^{-n} a_n J_n(k_1 r) \cos n\phi \quad (7c)$$

- the normal component of displacement of the fluid must be equal to the normal component of displacement of the solid at the surface  $r = a$

$$u_r^i + u_r^s = u_r \quad (8)$$

where the radial components of displacement of the incident and scattered fields are

$$u_r^i = \frac{1}{\rho_0 \omega^2} \frac{\partial p_i}{\partial r} = \frac{P_0}{\rho_0 \omega^2} \sum_{n=0}^{\infty} \varepsilon_n j^{-n} \frac{d}{dr} J_n(k_0 r) \cos n\phi \quad (9a)$$

$$u_r^s = \frac{1}{\rho_0 \omega^2} \frac{\partial p_s}{\partial r} = \frac{P_0}{\rho_0 \omega^2} \sum_{n=0}^{\infty} \varepsilon_n j^{-n} \frac{d}{dr} H_n^{(2)}(k_0 r) \cos n\phi \quad (9b)$$

and the radial component of displacement inside the cylinder is

$$u_r = -\frac{\partial U}{\partial r} + \frac{1}{r} \frac{\partial A_z}{\partial \phi} = P_0 \sum_{n=0}^{\infty} \varepsilon_n j^{-n} \left[ \frac{nb_n}{r} J_n(k_2 r) - a_n \frac{d}{dr} J_n(k_1 r) \right] \cos n\phi \quad (10)$$



where  $U$  and  $A_z$  are defined in (6).

- the tangential components of shearing stress must vanish at the surface  $r = a$

$$e_{r\phi} = e_{rz} = 0 \quad (11a)$$

where

$$e_{r\phi} = \frac{E}{2(1+\sigma)} \left[ \frac{1}{r} \frac{\partial u_r}{\partial \phi} + r \frac{\partial}{\partial r} \left( \frac{u_\phi}{r} \right) \right] \quad (11b)$$

$$e_{rz} = \frac{E}{2(1+\sigma)} \left[ \frac{\partial u_r}{\partial z} + \frac{\partial u_z}{\partial r} \right]. \quad (11c)$$

Inside the cylinder, the radial component of displacement is given in (10) and the angular component of displacement is

$$u_\phi = -\frac{1}{r} \frac{\partial U}{\partial \phi} - \frac{\partial A_z}{\partial r} = P_0 \sum_{n=0}^{\infty} \varepsilon_n j^{-n} \left[ \frac{na_n}{r} J_n(k_1 r) - b_n \frac{d}{dr} J_n(k_2 r) \right] \sin n\phi \quad (12)$$

By symmetry,  $e_{rz} = 0$  everywhere.

Using (1)–(12), one can solve for  $c_n$  to obtain

$$c_n = -\frac{J_n(x_0) + jY_n J_n'(x_0)}{H_n^{(2)}(x_0) + jY_n H_n^{(2)'}(x_0)} \quad (13)$$

where the specific acoustic admittance,  $Y_n$ , of the  $n^{\text{th}}$  partial-wave is

$$Y_n = \frac{2\rho x_0}{\rho_0 x_2^2} \frac{\left( \frac{\sigma}{1-2\sigma} + 1 - \frac{n^2}{x_1^2} \right) x_1^2 J_n(x_1) + x_1 J_n'(x_1) - n\Gamma_n J_n(x_2) + n\Gamma_n x_2 J_n'(x_2)}{n\Gamma_n J_n(x_2) - x_1 J_n'(x_1)} \quad (14)$$

and

$$\Gamma_n = \frac{2nx_1 J_n'(x_1) - 2nJ_n(x_1)}{(2n^2 - x_2^2) J_n(x_2) - 2x_2 J_n'(x_2)} \quad (15)$$

with  $x_p = k_p a$  for  $p = 0, 1$ , or  $2$ . Inserting the expression for  $\Gamma_n$  and rearranging terms yields

$$Y_n = jC \frac{\left[ \frac{1-\sigma}{1-2\sigma} + \frac{A_1}{x_1} - \frac{n^2}{x_1^2} \right] \left[ 1 + \frac{2A_2}{x_2} - \frac{2n^2}{x_2^2} \right] - \frac{2n^2}{x_1 x_2} \left( A_1 - \frac{1}{x_1} \right) \left( A_2 - \frac{1}{x_2} \right)}{A_1 \left[ 1 + \frac{2A_2}{x_2} - \frac{2n^2}{x_1 x_2^2 A_1} \right]} \quad (16)$$

where

$$C = \frac{2x_0x_1}{x_2^2} \frac{\rho_0}{\rho} = \frac{2k_0k_1}{k_2^2} \frac{\rho_0}{\rho} \quad (17)$$

independent of  $a$ , and  $A_i = J_n'(x_i)/J_n(x_i)$  for  $i = 1, 2$ . Equation (16) can be written as  $Y_n = CN/D$  where  $N$  and  $D$  represent the numerator and denominator, respectively.

In the limiting case of an acoustically hard medium,  $\mu \rightarrow \infty$  implying  $Y_n \rightarrow \infty$  and then

$$c_n = -\frac{J_n'(x_0)}{H_n^{(2)}(x_0)} \quad (18)$$

whereas for a soft medium,  $\mu \rightarrow 0$  implying  $Y_n \rightarrow 0$ , giving

$$c_n = -\frac{J_n(x_0)}{H_n^{(2)}(x_0)}. \quad (19)$$

### 3 IMPEDANCE BOUNDARY CONDITIONS

Having found the scattered field, the accuracy to which the field can be determined using impedance boundary conditions of different orders is now examined. The simplest (first order) impedance boundary condition can be written as

$$\frac{\partial p}{\partial n} + jk_0 Y p = 0 \quad (20)$$

where  $Y$  is a normalized admittance and  $n$  is in the direction of the outward normal to the surface. More generally, a boundary condition of order  $M > 1$  has the form

$$\frac{\partial p}{\partial n} = -jk_0 \left\{ \beta_0 + \sum_{m=1}^{M/2} (-1)^m \left[ \frac{\partial^m}{\partial s^m} \left( \beta_{11}^{(m)} \frac{\partial^m}{\partial s^m} + \beta_{12}^{(m)} \frac{\partial^m}{\partial t^m} \right) + \frac{\partial^m}{\partial t^m} \left( \beta_{21}^{(m)} \frac{\partial^m}{\partial s^m} + \beta_{22}^{(m)} \frac{\partial^m}{\partial t^m} \right) \right] \right\} p \quad (21)$$

where  $s$  and  $t$  are tangential variables [15, 16]. In the particular case of a two-dimensional body with no  $t$  dependence, this reduces to

$$\frac{\partial p}{\partial n} = -jk_0 \left\{ \beta_0 + \sum_{m=1}^{M/2} (-1)^m \beta_{11}^{(m)} \frac{\partial^{2m}}{\partial s^{2m}} \right\} p \quad (22)$$

and for a circular cylinder with  $n = r$  and  $s = r\phi$

$$\frac{\partial p}{\partial n} = -jk_0 \left\{ \beta_0 - \beta_{11}^{(1)} \frac{1}{r^2} \frac{\partial^2}{\partial \phi^2} + \beta_{11}^{(2)} \frac{1}{r^4} \frac{\partial^4}{\partial \phi^4} - \dots \right\} p \quad (23)$$

When applied to an eigenfunction expansion of  $p$  in the form  $\sum_n a(n) \cos n\phi$ , the corresponding admittance is

$$Y = \beta_0 + \beta_{11}^{(1)} \left(\frac{n}{r}\right)^2 + \beta_{11}^{(2)} \left(\frac{n}{r}\right)^4 + \dots \quad (24)$$

### 3.1 First Order IBC

Let  $x_i = N_i x_0$  ( $i = 1, 2$ ) where  $N_1$  and  $N_2$  are the complex refractive indices of the viscoelastic medium. If  $|x_i|$  are so large that terms  $\mathcal{O}(x_i^{-2})$  can be neglected,  $A_i$  can be approximated by the first two terms of the series given in (A.3), *i.e.*

$$A_i \simeq j \left( 1 - \frac{1}{2N_i j x_0} \right). \quad (25)$$

For a first order solution,  $N$  and  $D$  can be approximated by polynomials of order  $1/x$ :

$$N \simeq Z + \frac{K}{x}, \quad D \simeq 1 + \frac{P}{x}$$

where  $Z$ ,  $K$ , and  $P$ , the coefficients of the inverse power series, are determined in to be

$$Z = \frac{1 - \sigma}{1 - 2\sigma} \quad (26a)$$

$$K = -\frac{1}{N_1 j} - \frac{1 - \sigma}{1 - 2\sigma} \frac{2}{N_2 j} \quad (26b)$$

$$P = \frac{1}{2N_1 j} + \frac{2}{N_2 j}. \quad (26c)$$

Substituting the above expressions for  $Z$ ,  $K$ , and  $P$ , and neglecting terms of order  $\mathcal{O}(x^{-2})$  yields

$$Y \simeq C \left\{ \frac{1 - \sigma}{1 - 2\sigma} + \frac{j}{x_1} \left[ 1 - \frac{1}{2} \left( \frac{1 - \sigma}{1 - 2\sigma} \right) \right] \right\}. \quad (27)$$

Thus, for the first order solution,  $\beta_0$  of (24) is

$$\beta_0 = C \left\{ \frac{1 - \sigma}{1 - 2\sigma} \left( 1 + \frac{1}{2N_1 j x_0} \right) - \frac{1}{N_1 j x_0} \right\}. \quad (28)$$

To this order the admittance is mode *independent*.

### 3.2 Second Order IBC

If  $|x_i|$  are somewhat smaller, but still large enough to allow terms  $\mathcal{O}(x_i^{-4})$  to be neglected,  $A_i$  can be approximated by the first four terms of the series given in (A.3)

$$A_i \simeq j \left( 1 - \frac{1}{2N_i j x_0} - \frac{4n^2 - 1}{8N_i^2 x_0^2} + \frac{4n^2 - 1}{8N_i^3 j x_0^3} \right).$$

For a second order solution,  $N$  and  $D$  in (14) can be approximated by polynomials of order  $1/x^3$ :

$$N \simeq \left( Z + \frac{K}{x} + \frac{L}{x^2} + \frac{M}{x^3} \right)$$

$$D \simeq \left( 1 + \frac{P}{x} + \frac{Q}{x^2} + \frac{R}{x^3} \right)$$

where  $Z$ ,  $K$ , and  $P$  are defined in (26) and  $L$ ,  $M$ ,  $Q$ , and  $R$ , are

$$L = -\frac{2n^2 + 1}{2N_1^2} + \frac{2n^2 - 2}{N_1 N_2} - \frac{2n^2 + 1}{N_2^2} \frac{1 - \sigma}{1 - 2\sigma} \quad (29a)$$

$$M = \frac{4n^2 - 1}{8N_1^3 j} + \frac{4n^2 - 1}{4N_2^3 j} \frac{1 - \sigma}{1 - 2\sigma} - \frac{1}{N_1^2 N_2 j} (n^2 - 1) - \frac{1}{N_1 N_2^2 j} (n^2 - 1) \quad (29b)$$

$$Q = \frac{4n^2 - 3}{8N_1^2} - \frac{1}{N_1 N_2} - \frac{3}{N_2^2} \quad (29c)$$

$$R = -\frac{1}{8N_1^3 j} + \frac{4n^2 - 3}{4N_1^2 N_2 j} + \frac{4n^2 - 3}{2N_1 N_2^2 j} - \frac{4n^2 + 15}{4N_2^3 j}. \quad (29d)$$

Thus, for the second order boundary condition,  $\beta_0$  and  $\beta_{11}^{(1)}$  of (24) are

$$\beta_0 = C \left\{ \frac{1 - \sigma}{1 - 2\sigma} \left( 1 + \frac{1}{2N_1 j x_0} - \frac{3}{8N_1^2 x_0^2} - \frac{1}{8N_1^3 j x_0^3} \right) - \frac{1}{N_1 j x_0} \right\} \quad (30)$$

$$\beta_{11}^{(1)} = \frac{C}{2k_0^2} \left\{ \frac{1 - \sigma}{1 - 2\sigma} \left( \frac{1}{N_1^2} - \frac{4}{N_2^2} + \frac{2}{N_1^2 N_2 k_0 j} - \frac{8}{N_2^3 k_0 j} \right) - \frac{2}{N_1^2} + \frac{4}{N_1 N_2} - \frac{2}{N_1^3 j x_0} - \frac{4}{N_1^2 N_2 j x_0} + \frac{6}{N_1 N_2^2 j x_0} \right\} \quad (31)$$

Note that the second order solution has the requisite mode dependence.

#### 4 VALIDATION

In the far-field where  $r \gg a$ ,  $H_n^{(2)}(k_0 r)$  may be written in its asymptotic form

$$H_n^{(2)}(k_0 r) \sim \sqrt{\frac{2j}{\pi k_0 r}} j^n e^{-jk_0 r}, \quad (32)$$

and from (2) the far field pressure then becomes

$$p^s = -P_0 e^{-jk_0 r} \sqrt{\frac{2j}{\pi k_0 r}} \sum_{n=0}^{\infty} \varepsilon_n c_n \cos n\phi. \quad (33)$$

The scattering width (SW), or alternatively, the bistatic acoustic cross section per unit length  $\sigma$ , defined in [5] as

$$\sigma(\phi) = \lim_{r \rightarrow \infty} \left[ 2\pi r \left| \frac{p^s}{p^i} \right|^2 \right], \quad (34)$$

is now

$$\sigma(\phi) = \frac{2\lambda}{\pi} \left| \sum_{n=0}^{\infty} \varepsilon_n c_n \cos n\phi \right|^2 \quad (35)$$

with  $c_n$  given by (13).

Figure 2 shows the normalized monostatic SW ( $\phi = 0$ ) as a function of  $k_0 a$  for a lossy cylinder ( $\sigma = 1/3$ ,  $E=20$  MPa,  $N_1 = 2-j1.5$ ,  $N_2 = 2-j4$ , and  $\rho=1.81$  g/cm<sup>3</sup>) immersed in an inviscid fluid medium ( $c_0=1540$  m/s and  $\rho_0=1.06$  g/cm<sup>3</sup>) for the SIBC, the second order GIBC, and the exact normal-mode series solution computed using 31 modes. The parameter values approximate a rib embedded in a soft tissue background. The exact solution requires the evaluation of the specific acoustic admittance, and consequently, computation of many cylindrical functions for each  $n^{\text{th}}$  partial-wave solution at each frequency. In contrast, the SIBC and GIBC are calculated using the relatively simple inverse power series shown in (24) in conjunction with (13). Not surprisingly, neither boundary condition is accurate for small values of  $k_0 a$ , and do not pick up the effects corresponding to the first two shear wave resonances across the diameter of the cylinder. The higher order resonances are invisible because of the absorption, and as the absorption increases, the second and then the first resonances disappear.

The normalized monostatic SW percent error is plotted as a function of  $k_0a$  in Fig. 3 for (a)  $N_1 = 2 - j1.5$ ,  $N_2 = 2 - j4$  and (b)  $N_1 = 2 - j2$ ,  $N_2 = 2 - j8$ . In case (a), for an allowable error of 3%, the SIBC approximation is valid for  $k_0a > 13.7$  and the GIBC for the somewhat smaller values  $k_0a > 10.2$ . For an allowable error of 1%, the SIBC is valid for  $k_0a > 29.6$  and the GIBC for  $k_0a > 21.8$ . If the loss is increased as shown for case (b), the SIBC can be seen to be accurate to within 3% for  $k_0a > 4.85$  and the GIBC for  $k_0a > 4.28$  and to within 1% for  $k_0a > 9.59$  and the GIBC for  $k_0a > 7.34$ .

The normalized bistatic SW of a cylinder with  $k_0a = 8$ ,  $N_1 = 2 - j8$  and  $N_2 = 2 - j1$  for the SIBC, GIBC, and exact solution as shown in Fig. 4. Clearly, the GIBC more accurately models the angular variation of the scattered field than the SIBC, and this is particularly noticeable as the scattering angle  $\phi$  increases. The accuracy of the GIBC can be attributed to its ability to model some of the partial mode dependence of the specific acoustic admittance and to the inclusion of more terms representing the surface curvature. The former is the dominant effect, and the accuracy of the SIBC is unchanged if the  $\beta_0$  of (30) is used in place of (28).

## 5 CONCLUSIONS

In ultrasonic scattering by the bone-like structures, it is necessary to include the effect of the shear waves, and these significantly complicate the solution of a problem as fundamental as the scattering from an infinite circular cylinder. Since the structures are lossy, one way to simplify the problem is to invoke an impedance boundary condition, and this could make tractable the analytical or numerical determination of the scattering from other geometries. From the exact expression for the partial mode impedances for a circular cylinder, first and second order impedance boundary conditions were derived by asymptotic expansion for large  $k_0a$ . With each boundary condition the accuracy improves as  $k_0a$  increases, or as the absorption increases for a fixed  $k_0a$ , and for many purposes the accuracy of the SIBC may be adequate. Under all circumstances, however, the GIBC is more accurate primarily because of the mode dependence that it provides.

## ACKNOWLEDGMENT

The first author gratefully acknowledges the support of this research by the National Science Foundation through its Graduate Fellowship Program and thanks S. R. Legault for conversations regarding this work.

## APPENDIX

The Bessel function  $J_n(x)$  of order  $n$  can be expanded using an asymptotic series as shown in Bowman [5]:

$$J_n(x) = e^{j(x-n\pi/2)} \sqrt{\frac{2j}{\pi x}} \left\{ 1 - \frac{4n^2 - 1}{8jx} - \frac{(4n^2 - 1)(4n^2 - 9)}{128x^2} + \frac{(4n^2 - 1)(4n^2 - 9)(4n^2 - 25)}{128 \cdot 24jx^3} + \mathcal{O}(x^{-4}) \right\}. \quad (\text{A.1})$$

Accordingly,

$$J'_n(x) = j e^{j(x-n\pi/2)} \sqrt{\frac{2j}{\pi x}} \left\{ 1 - \frac{4n^2 + 3}{8jx} - \frac{(4n^2 - 1)(4n^2 + 15)}{128x^2} + \frac{(4n^2 - 1)(4n^2 - 9)(4n^2 + 35)}{128 \cdot 24jx^3} + \mathcal{O}(x^{-4}) \right\} \quad (\text{A.2})$$

and therefore

$$\frac{J'_n(x)}{J_n(x)} = j \left\{ 1 - \frac{1}{2jx} - \frac{4n^2 - 1}{8x^2} + \frac{4n^2 - 1}{8jx^3} + \mathcal{O}(x^{-4}) \right\}. \quad (\text{A.3})$$

## REFERENCES

- [1] G. E. Goldman and T. F. Heuter, "Tabular data of the velocity of high-frequency sound in mammalian tissue," *J. Acous. Soc. Amer.*, vol. 28, pp. 35–37, 1956.
- [2] P. N. T. Wells, *Biomedical Ultrasonics*, Academic Press, London, 1977.
- [3] R. C. Chivers, "Ultrasonic velocity and attenuation in mammalian tissues," *J. Acous. Soc. Amer.*, vol. 63, pp. 940–953, 1978.
- [4] J. P. Jones, "Quantitative characterization of tissue using ultrasound," *IEEE Trans. Nuclear Sci.*, vol. NS-27, no. 3, pp. 940–953, 1980.
- [5] J. J. Bowman, T. B. A. Senior, and P. L. E. Uslenghi, *Electromagnetic and Acoustic Scattering by Simple Shapes*, Harper and Row, London, revised edition, 1987.
- [6] J. J. Faran, "Sound scattering by solid cylinders and spheres," *J. Acous. Soc. Amer.*, vol. 23, no. 4, pp. 405–418, Jul 1951.
- [7] R. H. Vogt, L. Flax, L. R. Dragonette, and W. G. Neubauer, "Monostatic reflection of a plane wave from an absorbing sphere," *J. Acous. Soc. Amer.*, vol. 57, no. 3, pp. 558–561, Mar 1975.
- [8] R. H. Vogt, L. Flax, L. R. Dragonette, and W. G. Neubauer, "Erratum: Monostatic reflection of a plane wave from an absorbing sphere," *J. Acous. Soc. Amer.*, vol. 62, no. 5, pp. 1315, Nov 1977.
- [9] L. Flax and W. G. Neubauer, "Acoustic reflection from layered elastic absorptive cylinders," *J. Acous. Soc. Amer.*, vol. 61, no. 2, pp. 307–312, Feb 1977.
- [10] J. George and H. Überall, "Approximate methods to describe the reflections from cylinders and spheres with complex impedance," *J. Acous. Soc. Amer.*, vol. 65, no. 1, pp. 15–24, Jan 1979.
- [11] V. M. Ayres and G. C. Gaunaurd, "Acoustic resonance scattering by viscoelastic objects," *J. Acous. Soc. Amer.*, vol. 81, no. 2, pp. 301–311, Feb 1987.
- [12] J. R. Wait, "The scope of impedance boundary conditions in radio propagation," *IEEE Trans. Geosci. Remote Sensing*, vol. GE-28, no. 4, pp. 721–723, Jul 1990.
- [13] A. E. H. Love, *A Treatise on the Mathematical Theory of Elasticity*, Dover, New York, fourth edition, 1878.
- [14] P. M. Morse and H. Feshbach, *Methods of Theoretical Physics*, McGraw-Hill, London, 1953.
- [15] T. B. A. Senior, "Generalized boundary conditions for scalar fields," *J. Acous. Soc. Amer.*, vol. 97, no. 6, pp. 3473–3477, Jun 1995.
- [16] T. B. A. Senior and J. L. Volakis, *Approximate Boundary Conditions in Electromagnetics*, IEE Press, London, 1995.



TABLE I  
VARIOUS BIOLOGICAL PARAMETERS AT 1 MHz

Tissue	Speed ( $c$ ) [m s <sup>-1</sup> ]	Density ( $\rho$ ) [g cm <sup>-3</sup> ]	Impedance ( $Z$ ) [MPa s m <sup>-1</sup> ]	Absorption ( $\alpha$ ) [dB cm <sup>-1</sup> MHz <sup>-1</sup> ]
Blood	1570	1.06	1.61–1.62	0.18
Bone	3360–4080	1.38–1.81	3.75–7.80	13
Brain	1541	1.03	1.55–1.66	0.85
Fat	1450–1476	0.92	1.35–1.38	0.63
Kidney	–	1.04	1.62	–
Liver	1570–1585	1.06	1.64–1.68	–
Lung	650	0.40	0.26	41
Muscle	1568–1585	1.07	1.64–1.74	1.3–3.3
Spleen	–	1.06	1.65–1.67	–
Water	1480	1.00	1.48–1.52	0.0022
Air	343	–	0.000415	12
HST (mean)	1540	–	1.63	0.81

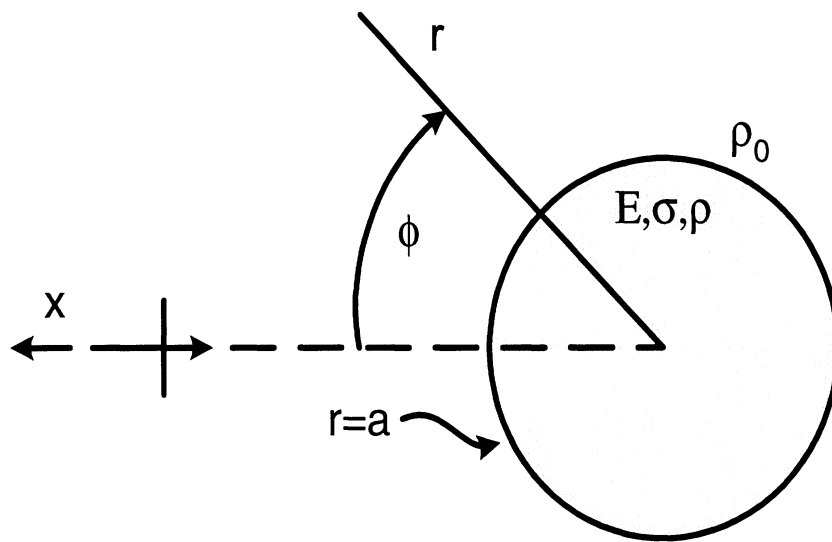


Fig. 1. Cross-sectional view of viscoelastic circular cylinder of radius  $a$  excited by plane acoustic wave

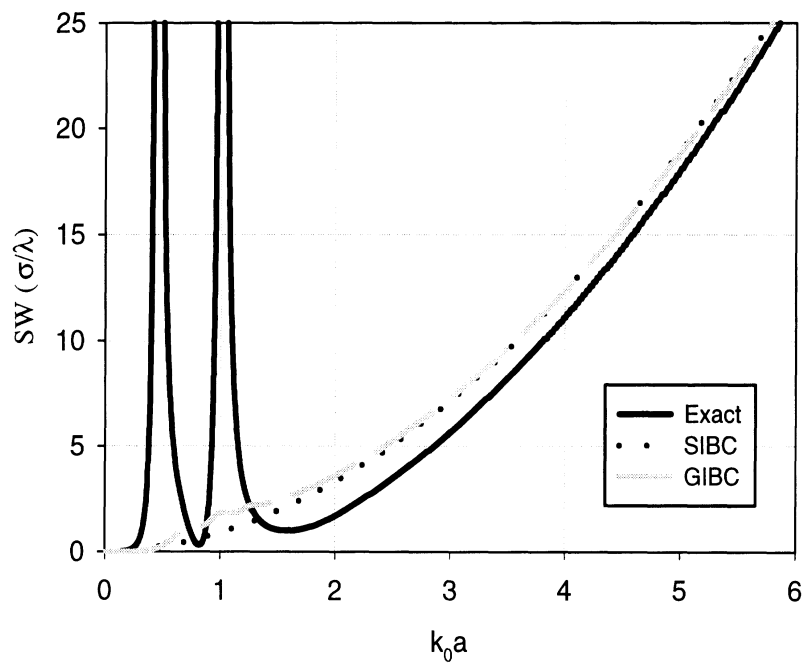


Fig. 2. Normalized monostatic SW as a function of  $k_0 a$  with  $N_1 = 2 - j1.5$ ,  $N_2 = 2 - j4$

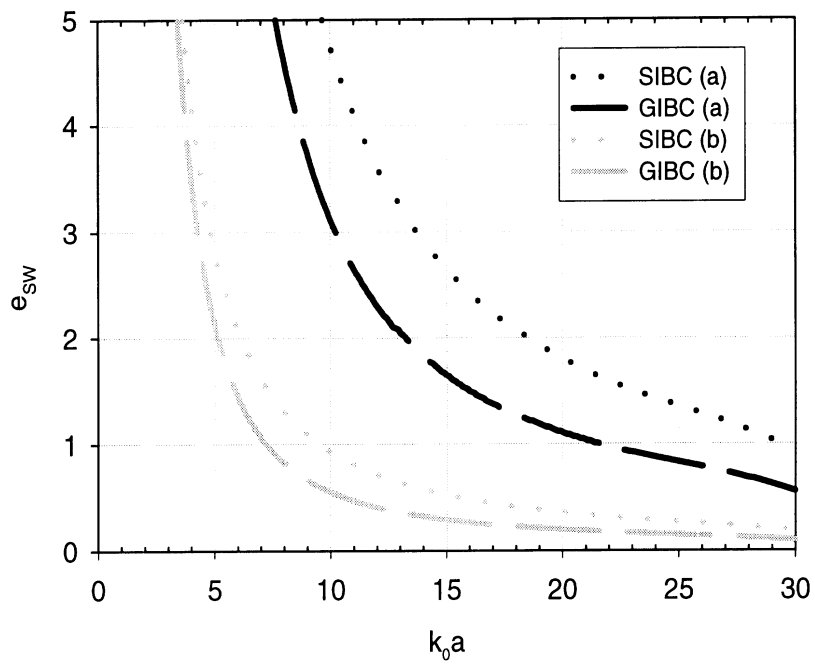


Fig. 3. Normalized monostatic SW percent error as a function of  $k_0 a$  for (a)  $N_1 = 2 - j1.5$ ,  $N_2 = 2 - j4$ , (b)  $N_1 = 2 - j2$ ,  $N_2 = 2 - j8$

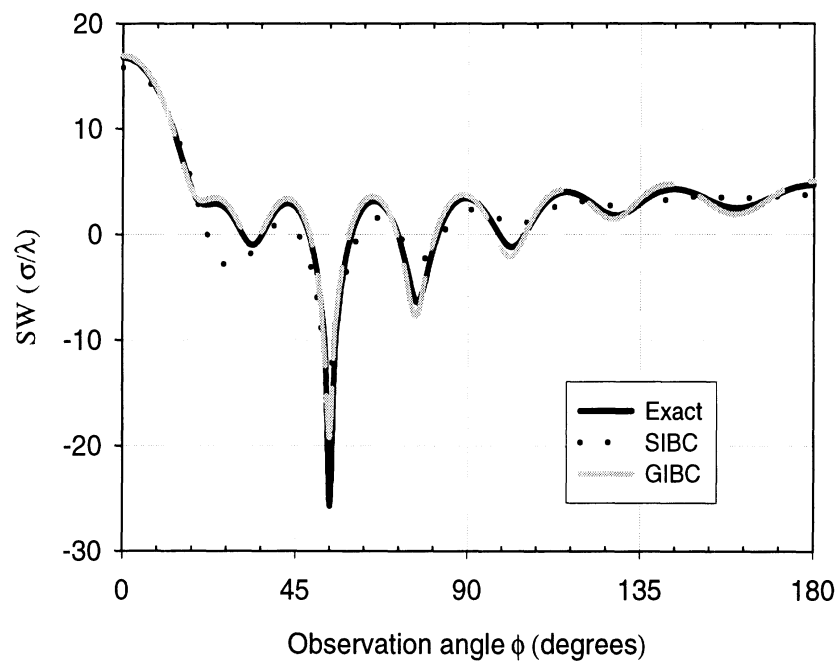


Fig. 4. Normalized bistatic SW of a cylinder with  $k_0 a = 8$ ,  $N_1 = 2 - j8$ , and  $N_2 = 2 - j1$